

Discrete diffraction and shape-invariant beams in optical waveguide arrays

Stefano Longhi

Dipartimento di Fisica and Istituto di Fotonica e Nanotecnologie del CNR, Politecnico di Milano, Piazza L. da Vinci 32, I-20133 Milano, Italy

(Received 16 January 2009; published 30 March 2009)

General properties of linear propagation of discretized light in homogeneous and curved waveguide arrays are comprehensively investigated and compared to those of paraxial diffraction in continuous media. In particular, general laws describing beam spreading, beam decay, and discrete far-field patterns in homogeneous arrays are derived using the method of moments and the steepest-descent method. In curved arrays, the method of moments is extended to describe evolution of global beam parameters. A family of beams which propagate in curved arrays maintaining their functional shape—referred to as discrete Bessel beams—is also introduced. Propagation of discrete Bessel beams in waveguide arrays is simply described by the evolution of a complex- q parameter similar to the complex- q parameter used for Gaussian beams in continuous lensguide media. A few applications of the q parameter formalism are discussed, including beam collimation and polygonal optical Bloch oscillations.

DOI: [10.1103/PhysRevA.79.033847](https://doi.org/10.1103/PhysRevA.79.033847)

PACS number(s): 42.79.Gn, 42.82.Et

I. INTRODUCTION

Linear and nonlinear propagation of “discretized” light in arrays of evanescently coupled optical waveguides has received a great and increasing interest in the past recent years (see, for instance, [1,2] and references therein). As compared to diffraction or refraction in continuous (nonstructured) media, discrete diffraction and refraction in waveguide arrays show rather uncommon effects which result from the evanescent coupling among adjacent waveguides forming a one-dimensional or a two-dimensional lattice. For instance, linear propagation of light waves in homogeneous arrays may show diffraction reversal and self-collimation effects [3,4], anomalous refraction [4], the discrete Talbot effect [5], and quasi-incoherent propagation [6], to name a few. Remarkably, discrete diffraction can be tailored by properly introducing inhomogeneities in the lattice or by varying its topology. In particular, since the first proposals and demonstrations of optical Bloch oscillations [7–9] and “diffraction management” in zigzag arrays [3], the use of waveguide arrays with curved optical axis has been extensively investigated both theoretically and experimentally, with the demonstration of diffraction suppression via Bloch oscillations [1,7–11] or dynamic localization [12,13], polychromatic diffraction management [14], astigmatic diffraction control [15], multicolor Talbot effect [14], and discrete soliton management [14,16]. Linear and nonlinear light propagations at the surface or at the interface of two waveguide lattices also exhibit a variety of interesting properties which have been investigated in several recent works (see, for instance, [2,17–19] and references therein). In spite of such a great amount of works, some facets of discrete diffraction, even in the simplest linear propagation regime, have been overlooked. Though in the linear regime the impulse response (Green’s function) of the array may be rather generally calculated analytically—in either straight or curved geometries and in presence or absence of boundaries—and its knowledge is enough to predict light evolution for any assigned initial excitation condition (see, for instance, [13,17]), some general issues of discrete diffrac-

tion, which are well known for paraxial propagation of beams in continuous media, have not been comprehensively addressed. These include: (i) a description of global beam parameter evolution in a closed analytical form; (ii) far-field discrete diffraction in homogeneous array (the analog of Fraunhofer diffraction in homogeneous continuous media); (iii) the general scaling law of beam broadening and beam decay, especially close to the self-collimation condition (also referred to as subdiffraction), which is commonplace for the more general class of photonic crystal structures (see, for instance, [20]); and (iv) the existence of shape-invariant discretized beams, i.e., special families of field distributions which—like Gaussian beams in continuous lensguide media—do propagate in straight or curved waveguide arrays maintaining their functional shape. It is the aim of this work to shed some light into such issues. In particular, it is shown rather generally that: (i) the scaling law describing broadening of discretized light in homogeneous arrays is the same as that of standard paraxial diffraction theory of homogeneous continuous media (beam size asymptotically grows linearly with propagation distance), independently of the precise array dispersion curve and even along self-collimation directions; (ii) in a homogeneous array, the discrete far-field pattern is not the (discrete) Fourier transform of the near-field distribution, and the scaling law of beam decay may depend on the observation angle; (iii) special field distributions, which propagate in straight or curved waveguide arrays maintaining their functional shape and referred to as “discrete Bessel beams,” can be introduced for simple tight-binding waveguide models; and (iv) a discrete Bessel beam is defined by a complex- q parameter, analogous to the one used for Gaussian beams in continuous lensguide media, and propagation of the q parameter along the array admits a simple geometric interpretation.

The paper is organized as follows. In Sec. II general properties of discrete diffraction in homogeneous waveguide arrays are presented, including the derivation of the general scaling laws of beam broadening and beam decay, and far-field discrete diffraction, with a note on self-collimation regimes. In Sec. III, some general rules of beam propagation in

curved waveguide arrays are derived within the nearest-neighbor coupling approximation, whereas in Sec. IV the family of shape-invariant discrete Bessel beams is introduced, together with the complex- q parameter formalism. Applications to beam collimation and polygonal optical Bloch oscillations are also presented. Finally, in Sec. V the main conclusions are outlined.

II. DISCRETE DIFFRACTION IN A HOMOGENEOUS WAVEGUIDE ARRAY

A. Continuous model of discrete diffraction

The starting point of our analysis is provided by a rather standard model describing linear propagation of monochromatic light waves along the z direction of a one-dimensional or two-dimensional array of waveguides in the single-band and tight-binding approximations. For instance, in a one-dimensional array such conditions are satisfied when the tilt of beams and waveguides at the input facet is less than the Bragg angle, so that the lowest-order band of the array is excited and beam propagation is primarily characterized by coupling between the fundamental modes of the waveguides. For a two-dimensional array, the relevant equations describing discrete diffraction in a single-band approximation read

$$i\dot{c}_{n,m} = - \sum_{l,r} \Delta_{n-l,m-r} c_{l,r} \quad (1)$$

where $c_{n,m}(z)$ is the complex amplitude of the fundamental waveguide mode at the lattice site $\mathbf{r}_{n,m} = n\mathbf{a} + m\mathbf{b}$ identified by the indices (n, m) , \mathbf{a} and \mathbf{b} are the lattice vectors of the unit cell, the dot denotes the derivative with respect to z , and $\Delta_{n,m} = \Delta_{m,n}^*$ are the coupling rates. In order to derive a general rule of beam broadening due to discrete diffraction, it is worth introducing a continuous field envelope $\psi(x, y, z)$ satisfying the scalar Schrödinger-type equation

$$i\partial_z \psi(\mathbf{r}, z) = H_0(\mathbf{p}) \psi(\mathbf{r}, z), \quad (2)$$

where $\mathbf{r} = (x, y)$, $\mathbf{p} = -i\nabla_{\mathbf{r}}$,

$$H_0(\mathbf{p}) \equiv - \sum_{n,m} \Delta_{n,m} \exp(-i\mathbf{r}_{n,m} \cdot \mathbf{p}), \quad (3)$$

and $\mathbf{r}_{n,m} = n\mathbf{a} + m\mathbf{b}$. Taking into account that $\exp(-i\mathbf{R} \cdot \mathbf{p}) \psi(\mathbf{r}, z) = \psi(\mathbf{r} + \mathbf{R}, z)$, it follows that the solution $c_{n,m}(z)$ to discrete equation (1) can be identified with $\psi(\mathbf{r} = n\mathbf{a} + m\mathbf{b}, z)$. The formulation of the discrete light propagation problem [Eq. (1)] as a continuous problem [Eq. (3)] is a well-established procedure in solid-state physics [21] which enables the use of certain analytical techniques, such as the method of moments, developed for the continuous Schrödinger equation or for the paraxial wave equation (see, for instance, [22,23]). In addition, the continuous model includes, as a particular case, the problem of paraxial diffraction in a homogeneous medium (e.g., in the vacuum), which is attained by simply assuming for the Hamiltonian $H_0(\mathbf{p})$, in place of Eq. (3), the (normalized) parabolic form

$$H_0(\mathbf{p}) = \frac{\mathbf{p}^2}{2}. \quad (4)$$

The normalization conditions $\int d\mathbf{r} |\psi(\mathbf{r}, z)|^2 = 1$ for Eq. (2) and $\sum_{n,m} |c_{n,m}(z)|^2 = 1$ for discrete problem (1) will be assumed in the following analysis.

B. General law for beam spreading: Moment analysis

Two global parameters describing beam propagation are the beam center of mass $\langle \mathbf{r} \rangle = \langle x \rangle \mathbf{u}_x + \langle y \rangle \mathbf{u}_y$, and the transverse beam spot sizes $w_x(z)$ and $w_y(z)$ defined by

$$\langle \mathbf{r} \rangle = \int d\mathbf{r} \mathbf{r} |\psi(\mathbf{r}, z)|^2, \quad (5)$$

$$w_x(z) = \sqrt{\langle x^2 \rangle - \langle x \rangle^2}, \quad (6)$$

$$w_y(z) = \sqrt{\langle y^2 \rangle - \langle y \rangle^2}, \quad (7)$$

where

$$\langle x^2 \rangle(z) = \int d\mathbf{r} x^2 |\psi(\mathbf{r}, z)|^2, \quad \langle y^2 \rangle(z) = \int d\mathbf{r} y^2 |\psi(\mathbf{r}, z)|^2. \quad (8)$$

Note that the above definitions hold for both continuous and discrete diffraction models. In the latter case, assuming $\psi(\mathbf{r}, z)$ to be a piecewise constant function in each cell of the lattice and taking $|\mathbf{a} \times \mathbf{b}| = 1$ for the area of the unit cell, the integral over \mathbf{r} may be replaced by a double sum over the cell indices n and m ; i.e., in the discrete model one has $\int d\mathbf{r} \rightarrow \sum_{n,m}$.

The evolution equations for \mathbf{r} and $w_{x,y}$ can be readily obtained in a closed form by writing a set of Ehrenfest equations for the expectation values of \mathbf{r} , x^2 , and y^2 , and of commutator operators that arise in the calculation. The expectation value $\langle A \rangle \equiv \int d\mathbf{r} \psi^*(\mathbf{r}, z) A(\mathbf{r}, \mathbf{p}) \psi(\mathbf{r}, z)$ of any operator $A(\mathbf{r}, \mathbf{p})$ (not necessarily self-adjoint) evolves according to

$$\frac{d\langle A \rangle}{dz} = -i\langle [A, H_0] \rangle \quad (9)$$

and the commutation relations

$$[\mathbf{r}, f(\mathbf{p})] = i\nabla_{\mathbf{p}} f, \quad [g(\mathbf{r}), \mathbf{p}] = i\nabla_{\mathbf{r}} g \quad (10)$$

hold for any functions $f(\mathbf{p})$ and $g(\mathbf{r})$. For $A = \mathbf{r}$, one obtains

$$\frac{d\langle \mathbf{r} \rangle}{dz} = \langle \nabla_{\mathbf{p}} H_0 \rangle, \quad \frac{d\langle \nabla_{\mathbf{p}} H_0 \rangle}{dz} = 0, \quad (11)$$

i.e.,

$$\langle \mathbf{r} \rangle(z) = \langle \mathbf{r} \rangle(0) + \langle \nabla_{\mathbf{p}} H_0 \rangle z, \quad (12)$$

which is the evolution equation of the beam center of mass. Note that the path followed by any beam is always straight, regardless of the specific form of H_0 or initial field distribution which just determines the transverse drift velocity $\langle \nabla_{\mathbf{p}} H_0 \rangle$ of the beam. To determine the evolution equation of

the beam spot size w_x , let us assume $A=x^2$, so that the following cascade of Eherenfest equations [Eq. (9)] is obtained:

$$\frac{d\langle x^2 \rangle}{dz} = \left\langle x \frac{\partial H_0}{\partial p_x} + \frac{\partial H_0}{\partial p_x} x \right\rangle, \quad (13)$$

$$\frac{d}{dz} \left\langle x \frac{\partial H_0}{\partial p_x} + \frac{\partial H_0}{\partial p_x} x \right\rangle = 2 \left\langle \left(\frac{\partial H_0}{\partial p_x} \right)^2 \right\rangle, \quad (14)$$

$$\frac{d}{dz} \left\langle \left(\frac{\partial H_0}{\partial p_x} \right)^2 \right\rangle = 0. \quad (15)$$

After integration, one obtains

$$\langle x^2 \rangle(z) = \langle x^2 \rangle(0) + \left\langle x \frac{\partial H_0}{\partial p_x} + \frac{\partial H_0}{\partial p_x} x \right\rangle z + \left\langle \left(\frac{\partial H_0}{\partial p_x} \right)^2 \right\rangle z^2, \quad (16)$$

where the expectation values on the right-hand side of Eq. (16) are calculated at $z=0$, i.e., for the initial beam distribution. From Eqs. (6), (12), and (16) the following evolution equation for the beam spot size w_x is then obtained:

$$w_x^2(z) = w_x^2(0) + \alpha_x z + \beta_x^2 z^2, \quad (17)$$

where we have set

$$\alpha_x = \left\langle \left(x - \langle x \rangle \right) \frac{\partial H_0}{\partial p_x} + \frac{\partial H_0}{\partial p_x} (x - \langle x \rangle) \right\rangle, \quad (18)$$

$$\beta_x^2 = \left\langle \left(\frac{\partial H_0}{\partial p_x} \right)^2 \right\rangle - \left(\left\langle \frac{\partial H_0}{\partial p_x} \right\rangle \right)^2. \quad (19)$$

The expectation values are calculated at $z=0$. A similar expression for $w_y(z)$ can be obtained by replacing x with y in Eqs. (17)–(19). A major result expressed by Eq. (17) is that, regardless of the particular form of H_0 , $w_x(z)$ [and similarly $w_y(z)$] asymptotically grows with z linearly, with a diffraction length given by $\sim 1/\beta_x$. Therefore—and this one of the major results of this section—the broadening law of a spatial beam due to diffraction does not differ for discrete or continuous diffraction. In addition, for a beam carrying a finite power and admitting finite moments $\langle x^2 \rangle$ and $\langle y^2 \rangle$, the coefficient β_x^2 given by Eq. (19) is always strictly positive and does not vanish. This can be generally proven by observing that β_x^2 is the variance of the operator $(\partial H_0/\partial p_x)$, which is always positive and vanishes solely when the initial field distribution $\psi(x, y, 0)$ is an eigenfunction of $(\partial H_0/\partial p_x)$, i.e., of $p_x = -i\partial_x$. Since such eigenfunctions are delocalized plane waves, it then follows that the variance of $(\partial H_0/\partial p_x)$ is strictly positive for any initial beam distribution carrying a finite power, regardless of the specific form of H_0 .

C. Self-collimation regime

Beam self-collimation (also referred to as beam subdiffraction) is a well-known phenomenon occurring in homogeneous arrays and, more generally, in photonic crystal structures with engineered band structure $H_0(\mathbf{p})$ showing points of local flatness (see, for instance, [20]). The simplest ex-

ample of subdiffraction is the “arrest” of beam spreading in a one-dimensional tight-binding lattice with nearest-neighbor couplings, which was observed in Ref. [4] using relatively broad Gaussian beams at an incidence angle set in correspondence of an inflection point of the band dispersion curve. Though it is well understood that in such a regime diffraction is canceled solely at low orders, it was perhaps overlooked the fact that self-collimation *does not* modify the beam broadening scaling law [Eq. (17)]. In other words, self-collimation will correspond to a reduction in the coefficient β_x^2 for special initial field distributions, but *not* to a change in the scaling law describing beam broadening. If we consider, for the sake of simplicity, a one-dimensional lattice and assume that the spectrum $F(k)$ of the exciting beam, defined as $F(k) = 1/(2\pi) \int dx \psi(x, 0) \exp(-ikx)$, is narrow at around its mean k_0 , the value of β_x^2 , as given by Eq. (19), can be expanded in series of moments $I_l = \int dk (k - k_0)^l |F(k)|^2$ ($l = 2, 3, 4, \dots$) as

$$\beta_x^2 = b_2^2 I_2 + b_2 b_3 I_3 + \frac{1}{12} (4b_2 b_4 + 3b_3^2) I_4 - \frac{b_3^2}{4} I_2^2 + \dots, \quad (20)$$

where b_l is the value of the derivative $(\partial H_0/\partial k^l)$ evaluated at $k=k_0$. As I_l rapidly goes to zero as the order l increases, Eq. (20) shows that at the points k_0 of the dispersion curve where b_2 (and possibly b_3, b_4, \dots) vanishes beam broadening is reduced. We will refer to such points, where the dispersion curve $H_0(k)$ is locally flat, to as self-collimation points [note that the condition $H_0'(k_0)=0$ is not requested].

As an example, let us consider the simplest one-dimensional waveguide array in the nearest-neighbor approximation, considered in Ref. [4] to demonstrate self-collimation effects. The Hamiltonian H_0 has the form $H_0 = -2\Delta \cos(p)$, and the self-collimation points are located at $p = \pm \pi/2$. From Eq. (19) one obtains

$$\beta_x^2 = 2\Delta^2 \left[1 - \text{Re} \left(\sum_n c_n^* c_{n+2} \right) \right] + \Delta^2 \left[\sum_n c_n^* (c_{n+1} - c_{n-1}) \right]^2. \quad (21)$$

For a bell-shaped (e.g., Gaussian-shaped) and flat beam incident onto the array at a given tilting angle θ (normalized to the Bragg angle), we may write $c_n = |c_n| \exp(-i\pi\theta n)$, and one obtains

$$\beta_x^2(\theta) = 2\Delta^2 [1 - \kappa_1^2 + (\kappa_1^2 - \kappa_2) \cos(2\pi\theta)], \quad (22)$$

where κ_1 and κ_2 are defined by

$$\kappa_1 = \sum_n |c_n c_{n+1}|, \quad \kappa_2 = \sum_n |c_n c_{n+2}|. \quad (23)$$

Generally, it turns out that $\kappa_1^2 > \kappa_2$, so that the minimum of β_x is attained at $\theta = \pm 1/2$, i.e., at the self-collimation points as expected from Eq. (20). Conversely, the maximal diffraction (maximum value of β_x) is attained at normal incidence ($\theta=0$). The ratio between the minimum and maximum values of β_x , given by

$$\Gamma = \frac{\beta_x(\theta=1/2)}{\beta_x(\theta=0)} = \sqrt{\frac{1 + \kappa_2 - 2\kappa_1^2}{1 - \kappa_2}}, \quad (24)$$

may get very small for a broad input beam. To illustrate this point, let us consider as an example the following beam distribution at the input plane: $|c_n| = \mathcal{N}\alpha^{|n|}$, where the parameter α ($0 < \alpha < 1$) determines the spot size of the input beam ($\alpha \rightarrow 0$ for single waveguide excitation, and $\alpha \rightarrow 1$ for a plane-wave excitation), and $\mathcal{N} = [(1 - \alpha^2)/(1 + \alpha^2)]^{1/2}$ is a normalization factor. For such a field distribution, the values of coefficients κ_1 and κ_2 can be evaluated in a closed form, and read

$$\kappa_1 = \frac{2\alpha}{1 + \alpha^2}, \quad \kappa_2 = \frac{\alpha^2(3 - \alpha^2)}{1 + \alpha^2}. \quad (25)$$

The ratio Γ between the diffraction parameters at subdiffractive ($\theta=1/2$) and normal-incidence ($\theta=0$) regimes takes then the form [see Eq. (24)] $\Gamma = [(1 - \alpha^2)/(1 + \alpha^2)]^{1/2}$. Note that for a very broad beam excitation ($\alpha \rightarrow 1$), both κ_1 and κ_2 get close to 1, β_x tends to vanish [see Eq. (22)], and the diffraction length $\sim 1/\beta_x$ diverges independently of beam tilting angle θ , as expected for a very broad input beam. However, in this case the ratio of diffraction lengths in the normal ($\theta=0$) and subdiffractive ($\theta=1/2$) regimes, which scales as $\sim \Gamma$, tends to vanish as $\Gamma \sim (1 - \alpha)^{1/2}$. Conversely, for a very narrow input beam ($\alpha \rightarrow 0$), both κ_1 and κ_2 vanish and the diffraction length $\sim 1/\beta_x$ turns out to be independent of tilting angle and given by $\sim 1/(\sqrt{2}\Delta)$ [see Eq. (22)] as expected for single waveguide excitation.

D. Discrete far-field pattern and anomalous beam decay

In spite of the fact that the asymptotic law describing beam broadening due to diffraction is the same for discrete and continuous media, a deep difference is found when analyzing the decay behavior of the field intensity versus propagation distance and the far-field diffraction patterns. For the sake of simplicity, we will consider the diffraction problem in one dimension, though the results may be generalized to the two-dimensional diffraction problem. We then rewrite Eq. (2) as

$$i\partial_z\psi(x, z) = H_0(p)\psi(x, z), \quad (26)$$

where $p = p_x = -i\partial_x$. For the usual paraxial one-dimensional diffraction problem in a homogeneous continuous medium, one has $H_0(p) = p^2/2$, whereas for discrete diffraction in a one-dimensional waveguide array one has $H_0(-p) = H_0(p)$ ($-\pi \leq p < \pi$) and $H'_0(p) = 0$ at $p = 0$ and at the band edges $p = \pm \pi$. The most general solution to Eq. (26) can be written as

$$\psi(x, z) = \int dk F(k) \exp[ikx - iH_0(k)z], \quad (27)$$

where the spectrum $F(k)$ is determined by the beam distribution at the input plane $\psi(x, 0)$,

$$F(k) = \frac{1}{2\pi} \int dx \psi(x, 0) \exp(-ikx) \quad (28)$$

[$\int dx \rightarrow \sum_n$, $x \rightarrow n$, and $\psi(x=n) \rightarrow c_n$ in the discrete diffraction problem]. Our aim is to calculate the decay behavior of the field amplitude $\psi(x, z)$ as the propagation distance z increases, either at a constant x position (for instance, at $x=0$) or along a line $x = \alpha z$, where α is a constant parameter defining the ‘‘observation angle’’ of the diffracted pattern. Note that, as the observation angle α is varied, the function $\psi_0(\alpha; z) = \psi(x = \alpha z, z)$ corresponds, for large values of z , to the far-field diffraction pattern. We need thus to calculate the asymptotic behavior of the integral

$$\psi_0(\alpha; z) = \int dk F(k) \exp[izg(k)] \quad (29)$$

for $z \rightarrow \infty$, where we have set

$$g(k) = \alpha k - H_0(k). \quad (30)$$

For this purpose, we may use the methods of stationary phase or steepest descent (see, for instance, [24]), which predict that the asymptotic behavior of $\psi_0(\alpha; z)$ as $z \rightarrow \infty$ depends on the existence and of the order of stationary points of the phase $g(k)$ inside the integration domain.

Let us first consider the continuous diffraction problem, $H_0(p) = p^2/2$, and rederive the well-known result that the amplitude $\psi_0(\alpha; z)$ decays as $\sim 1/\sqrt{z}$ for any observation angle α and the far-field pattern is proportional to the Fourier spectrum of the input (near-field) distribution. In this case, $g(k) = \alpha k - k^2/2$ has a unique saddle point at $k = k_0 = \alpha$, with $g''(k_0) = -1 \neq 0$. Therefore, provided that the spectrum $F(k)$ has a nonvanishing component at $k = k_0$ and $F(k_0)$ does not diverge [25], according to the method of steepest descent one has

$$\psi_0(\alpha; z) \sim F(\alpha) \sqrt{\frac{2\pi}{z}} \exp[iz\alpha^2/2 - i\pi/4] \quad (31)$$

as $z \rightarrow \infty$. From Eq. (31) we obtain the well-known result of paraxial diffraction theory that the amplitude $\psi_0(\alpha; z)$ of the beam decays as $\sim 1/\sqrt{z}$ for any observation angle α [25], and that the far-field diffraction pattern is shaped as the Fourier spectrum $F(\alpha)$ of the near-field distribution. This scaling law may be referred to as the *normal* scaling law, in the sense that the beam intensity $I \propto |\psi|^2$ decays as $\sim 1/z$, whereas the beam spot size w_x increases asymptotically as $\sim z$ [see Eq. (17)], the product Iw_x being constant according to the power conservation law.

For the discrete diffraction problem, we prove now that the decay law is generally *slower* than $\sim 1/\sqrt{z}$ at the observation angles corresponding to self-collimation, and that the far-field pattern is peaked at such angles and does not reproduce the spectrum F of the near-field distribution. To this aim, let us observe that, according to the steepest-descent method, the slowest decay term in the integral of Eq. (29) comes from the saddle points $g'(k_0) = 0$ of largest order. In particular, if k_0 is a saddle point of order $n \geq 2$, i.e., $g(k) \approx g(k_0) + [g^{(n)}(k_0)/n!](k - k_0)^n$ for k close to k_0 [$g^{(n)}(k_0) \neq 0$],

the contribution of the saddle point to the integral in Eq. (29) for large values of z is given by [24]

$$\psi_0(\alpha; z) \sim \frac{F(k_0)}{|zg^{(n)}(k_0)|^{1/n}} (n!)^{1/n} \Gamma\left(\frac{1}{n}\right) \exp\left[izg(k_0) \pm i\frac{\pi}{2n}\right]. \quad (32)$$

Therefore, the decay law for $\psi_0(\alpha; z)$ scales as $\sim z^{-1/n}$, where n is the highest order of the saddle points of $g(k)$, provided that $F(k_0) \neq 0$. In the case of diffraction in a homogeneous continuous medium, the order of saddle point is always $n=2$. To determine n for the discrete diffraction problem, let us note that the dispersion curve $H_0(k)$ admits at least a couple of inflection points, say at $k=\pm k_0$, at which $H_0''(k_0)=0$. These points correspond to the self-collimation directions introduced in Sec. II C. Since $g'(k)=\alpha-H_0'(k)$, the inflection points $k=\pm k_0$ turn out to be also saddle points when the observation angle α is chosen equal to $H_0'(\pm k_0)$. Therefore, for the discrete diffraction problem the largest order n of saddle points is at least $n=3$, and the decay law of $\psi_0(\alpha; z)$, at the two observation angles $\alpha=\pm H_0'(k_0)$ corresponding to the self-collimation directions $\pm k_0$, is slowed down—as compared to continuous diffraction—to (at least) $\sim z^{-1/3}$. More generally, if the dispersion curve $H_0(k)$ of the lattice is engineered to achieve a very flat behavior near a self-collimation point $k=k_0$, with $g''(k_0)=g'''(k_0)=\dots=g^{(n-1)}(k_0)=0$ and $g^{(n)}(k_0) \neq 0$ ($n \geq 3$), the decay law of $\psi_0(\alpha; z)$ scales as $\sim z^{-1/n}$ at the observation angle $\alpha=H'(k_0)$. This scaling law of beam decaying in the discrete diffraction problem is therefore *anomalous*, in the sense that along the self-collimation directions the intensity decays slower than $1/z$, i.e., of the characteristic decay law that one might expect from power conservation arguments. This seemingly paradoxical circumstance may be solved by observing that for an observation angle α different from any of the self-collimation directions, the decay of $\psi_0(\alpha; z)$ may be either normal (i.e., $\sim 1/\sqrt{z}$) or even *faster*. More precisely, for a fixed value of α in modulus larger than $\alpha_{\max}=\max_k |H_0'(k)|$, the function $g(k)$ given by Eq. (30) does not have saddle points on the real axis, and $\psi_0(\alpha; z)$ decays as $\sim 1/z$. Conversely, for $|\alpha| < \alpha_{\max}$ the equation $g'(k)=\alpha-H_0'(k)=0$ admits at least one solution, with $g''(k) \neq 0$ for a second-order saddle point. In this case, according to the method of stationary phase the asymptotic behavior of $\psi_0(\alpha; z)$ for large values of z follows the normal law $\sim 1/\sqrt{z}$. To summarize, $\psi_0(\alpha; z)$ scales as $\sim F(k_0)z^{-1/n}$ at a self-collimation direction α , where $H_0'(k_0)=\alpha$ and k_0 is a saddle point of order $n \geq 3$; as $\sim F(k_0)z^{-1}$ for an observation angle α outside the “diffraction cone” $|\alpha| > \alpha_{\max}$; and as $\sim F(k_0)z^{-1/2}$ inside the diffraction cone region $|\alpha| < \alpha_{\max}$ but far from a self-collimation direction. The far-field pattern of discrete diffraction tends therefore to confine light inside the diffraction cone $|\alpha| \leq \alpha_{\max}$ with asymptotic peaks at the propagation directions corresponding to the angles of self-collimation.

This very general behavior may be illustrated more in detail for the case of a tight-binding lattice in the nearest-neighbor approximation considered in Sec. II C, for which $H_0(k)=-2\Delta \cos k$. In this lattice model one has $g'(k)=\alpha-2\Delta \sin k$ and $g''(k)=-2\Delta \cos k$, so that the angle of diffrac-

tion cone is given by $\alpha_{\max}=2\Delta$. Two saddle points of second order are found at $k=k_0=\pm \pi/2$ for the observation angles $\alpha=\pm \alpha_{\max}$, i.e., at the edge of the diffraction cone, at which the far-field discrete diffraction pattern is thus expected to show two peaks. For an observation angle α *strictly* inside the diffraction cone ($|\alpha| < 2\Delta$), the equation $g'(k)=0$ has two solutions which are saddle points of first order since $g''(k) \neq 0$. The main contribution to the integral on the right-hand side of Eq. (29) comes from these two saddle points, and can be calculated by the method of stationary phase, yielding explicitly

$$\begin{aligned} \psi(\alpha; z) &\sim \sqrt{\frac{i\pi}{z\sqrt{\Delta^2 - (\alpha/2)^2}}} \{-iF(k_0)\exp[i\alpha k_0 z \\ &\quad + 2i\Delta z \cos k_0] + F(\pi - k_0)\exp[i\alpha z(\pi - k_0) \\ &\quad - 2i\Delta z \cos k_0]\}, \quad \alpha > 0, \\ \psi(\alpha; z) &\sim \sqrt{\frac{i\pi}{z\sqrt{\Delta^2 - (\alpha/2)^2}}} \{-iF(-k_0)\exp[-i\alpha k_0 z \\ &\quad + 2i\Delta z \cos k_0] + F(-\pi + k_0)\exp[i\alpha z(-\pi + k_0) \\ &\quad - 2i\Delta z \cos k_0]\}, \quad \alpha < 0, \end{aligned} \quad (33)$$

where k_0 is the solution to the equation $\sin k_0=|\alpha/2\Delta|$ in the interval $0 \leq k_0 < \pi/2$. It should be noted that the far-field discrete diffraction pattern given by Eq. (33) holds for $|\alpha| < 2\Delta$. As $|\alpha|$ approaches 2Δ from below, the two saddle points of second order coalesce into a single saddle point of third order. This explains the divergence of Eq. (33) as $|\alpha| \rightarrow 2\Delta$, i.e., at the self-collimation directions, where the decay is slower and scales as $\sim z^{-1/3}$. For $|\alpha| > 2\Delta$, i.e., outside the diffraction cone, there are no saddle points on the real axis and the decay is faster and scales as $\sim 1/z$. An example of far-field discrete diffraction for a beam with a Gaussian spectrum $F(k) \sim \exp[-(k/w_k)^2]$ ($-\pi \leq k < \pi$) is shown in Fig. 1. In Fig. 1(a) the intensity distribution $|\psi(x, z)|^2$, as obtained by accurate numerical computation of the integral entering in Eq. (27), is plotted for a few propagation distances z . For the sake of readability, at each propagation distance z the field intensity has been normalized to its peak value. The diffraction cone and the emergence of two intensity peaks at the self-collimation directions $\alpha=\pm \alpha_{\max}$ are clearly visible just after a propagation distance z of ~ 10 – 20 times the coupling length $1/\Delta$ [Fig. 1(a)]. Inside the diffraction cone, the intensity distribution at such propagation distances is very well fitted by the analytical far-field distribution given by Eq. (33), as shown in Fig. 1(b). At much longer propagation distances, the self-collimation peaks become dominant, and the appearance of three different scaling laws of beam decay (fast decay outside the diffraction cone $|x| > 2\Delta z$; normal decay inside the diffraction cone $|x| < 2\Delta z$; and slower decay at the self-collimation directions $x=\pm 2\Delta z$) is very clearly visible, as shown in Fig. 1(c).

III. BEAM PROPAGATION IN CURVED WAVEGUIDE ARRAYS

Discrete diffraction of light waves in linear optical waveguide arrays can be controlled by introducing transverse in-

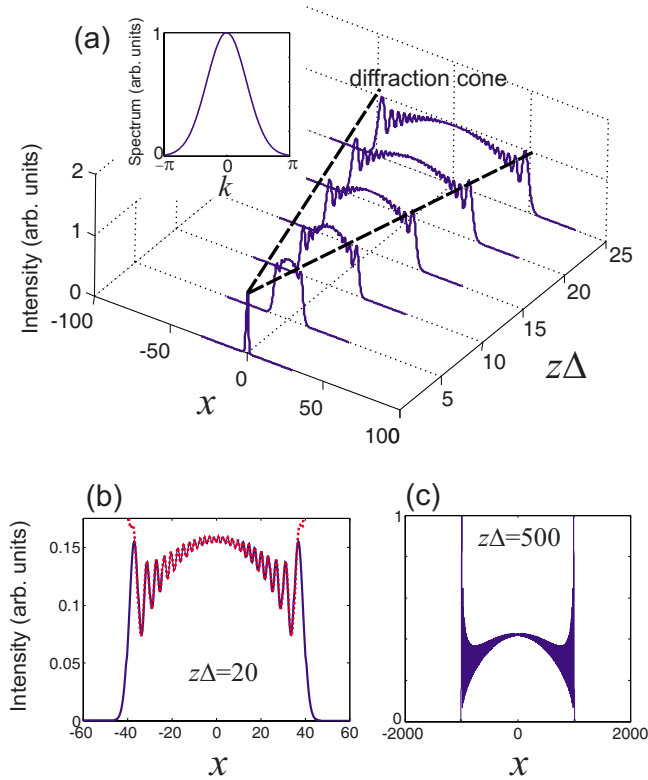


FIG. 1. (Color online) Beam propagation in a one-dimensional tight-binding lattice with nearest-neighbor coupling terms, showing far-field properties of discrete diffraction. In (a) the intensity distributions $|\psi(x, z)|^2$ are plotted, in arbitrary units, for propagation distances $z=0$, $z=5/\Delta$, $z=10/\Delta$, $z=15/\Delta$, $z=20/\Delta$, and $z=25/\Delta$, where Δ is the coupling rate between adjacent waveguides. The inset of (a) shows the Gaussian spectrum $F(k)$ of the beam ($w_k = 1.5$). In (c) the intensity distribution $|\psi(x, z)|^2$ is depicted for a propagation distance $z=20/\Delta$ as numerically calculated by Eq. (27) (solid curve) and by approximate relation (33) (dotted curve, almost overlapping with the solid one). In (c) the beam intensity is plotted at a propagation distance $z=500/\Delta$, clearly showing the dominance of two peaks at the diffraction cone edges (self-collimation directions) and the onset of three different decay laws at $|\alpha| > 2\Delta$, $\alpha = \pm 2\Delta$, and $|\alpha| < 2\Delta$.

dex gradients or local phase slips, which may produce a kind of refocusing or reimaging of beam distributions along the propagation distances (see, for instance, [3,9,12,13,26]), similar to what happens to light propagating in continuous lensguide media. In particular, waveguide arrays with a curved axis provide a particularly interesting setup for managing discrete diffraction for both monochromatic and polychromatic light [9,12–15]. It is therefore of major interest to have general laws describing the global behavior of beam propagation in curved waveguide arrays. In addition, it is well known that for the problem of paraxial diffraction in homogeneous continuous media or, more generally, of paraxial propagation in elementary optical systems and lensguides, one can introduce special families of field distributions (such as the Gaussian beams) that propagate maintaining unchanged their functional shape (shape-invariant beams), and that field propagation may be simply described by means of algebraic equations ruling out the evolution of

some complex-valued beam parameters (such as the complex- q parameter for Gaussian beams; see, for instance, [27]). A natural question is whether one can similarly introduce shape-invariant discrete beams, i.e., field distributions that do not change their functional shape when propagating along curved waveguide arrays. As the problem of discrete diffraction in waveguide arrays with curved axis or transversely imposed index gradients is analogous to the problem of one-dimensional or two-dimensional Bloch oscillations of electrons in periodic potentials with an applied electric field or of cold atoms in optical lattices, some results are already available in the literature. In particular, in recent works [28–30] an algebraic approach has been developed, capable of providing rather general results for wave-packet center-of-mass evolution and wave-packet spreading in certain lattice models. In this approach, after the introduction of a dynamical Lie algebra, an explicit form of the evolution operator is first derived, and then the expectation values of operators are calculated in the Heisenberg picture. However, the question of existence of shape-invariant discrete beams and of their propagation in curved waveguide arrays does not seem to have been addressed yet. In this section, we present a generalization of Eqs. (12) and (17) describing the evolution of beam center of mass and beam width in curved waveguide arrays using the method of moments. Though similar results were previously published in Refs. [28–30] using an algebraic operator approach, they are here rederived for the sake of completeness using the method of moments, which does not require the explicit calculation of the evolution operator and the formulation of the problem in terms of a Lie algebra. In Sec. IV a family of shape-invariant discrete beams will be introduced, proving that their propagation in a generally curved waveguide array is simply described by the evolution of a complex- q beam parameter, which plays an analogous role of, e.g., the complex- q parameter of Gaussian beams propagating in paraxial continuous optical systems.

Let us consider monochromatic light propagation in a two-dimensional waveguide array with a curved axis described by the parametric equations $x=x_0(z)$ and $y=y_0(z)$. The coupled-mode equations describing light transfer among coupled waveguides in the single-band and tight-binding approximations are an extension of Eq. (1) including fictitious transverse index gradients induced by waveguide curvature and read explicitly

$$i\dot{c}_{n,m} = - \sum_{l,r} \Delta_{n-l,m-r} c_{l,r} - \mathcal{E}(z) \cdot \mathbf{r}_{n,m}, \quad (34)$$

where $\mathcal{E}(z) = \mathcal{E}_x(z)\mathbf{u}_x + \mathcal{E}_y(z)\mathbf{u}_y$, $\mathcal{E}_x(z) = -(n_s/\lambda)\ddot{x}_0(z)$, $\mathcal{E}_y(z) = -(n_s/\lambda)\ddot{y}_0(z)$, n_s is the refractive index of the waveguide substrate, and $\lambda = \lambda/(2\pi)$ is the reduced wavelength of light. It should be noticed that the transverse index gradient entering in Eq. (34) may be also realized by applying a thermal gradient, or may describe lumped phase gradients [26] or an abrupt tilt of waveguide axis direction [3], cases in which $\mathcal{E}(z)$ shows a deltalike behavior. After introduction of a continuous function $\psi(\mathbf{r}, z)$ such that $\psi(\mathbf{r}_{n,m}, z) = c_{n,m}(z)$, one can readily check that discrete diffraction equations (34) are equivalent to the continuous Hamiltonian problem

$$i\partial_z\psi(\mathbf{r},z) = H(\mathbf{r},\mathbf{p})\psi(\mathbf{r},z), \quad (35)$$

where $\mathbf{p} = -i\nabla_{\mathbf{r}}$, with Hamiltonian

$$H = H_0(\mathbf{p}) - \mathcal{E}(z) \cdot \mathbf{r}, \quad (36)$$

where H_0 is the Hamiltonian of the homogeneous array defined by Eq. (3). The laws governing the evolution of beam center of mass and beam variance can be obtained by extending the method of moments described in Sec. II B for the free diffraction problem. In general, the cascade of equations that one obtains by applying Ehrenfest equation (9) to $\langle \mathbf{r} \rangle$, $\langle x^2 \rangle$, and $\langle y^2 \rangle$ —and to the commutators found throughout the calculations—turns out to be unlimited for a general form of H_0 , and a closed set of equations are found solely for special forms of H_0 . Such a special circumstance is encountered in case of a one-dimensional waveguide array in the nearest-neighbor approximation, and in case of a rectangular-lattice waveguide array neglecting diagonal interactions. The first model corresponds to the Hamiltonian

$$H(x,p) = -2\Delta \cos p - \mathcal{E}_x(z)x, \quad (37)$$

where Δ is the coupling rate between adjacent waveguides, and $p = p_x = -i\partial_x$. The second model, which has been, for instance, considered in the experiment of Ref. [31], is described by the Hamiltonian

$$H(\mathbf{r},\mathbf{p}) = -2\Delta_x \cos(p_x) - 2\Delta_y \cos(p_y) - \mathcal{E}_x(z)x - \mathcal{E}_y(z)y, \quad (38)$$

where Δ_x (Δ_y) is the coupling rate between adjacent horizontal (vertical) waveguides of the lattice [32].

A. One-dimensional array

Application of the moment method to one-dimensional Hamiltonian model (37) yields a set of closed coupled equations for the expectation values of operators x and θ , and of x^2 , ρ , and σ , where

$$\theta = \exp(ip), \quad (39)$$

$$\rho = \frac{1}{2}\{1 - \exp(-2ip)\}, \quad (40)$$

$$\sigma = i\{x \exp(-ip) + \exp(-ip)x\}. \quad (41)$$

Successive applications of Ehrenfest equation (9) yield for $\langle x \rangle$ and $\langle \theta \rangle$ the equations

$$\frac{d\langle x \rangle}{dz} = 2\Delta \operatorname{Im}(\langle \theta \rangle), \quad (42)$$

$$\frac{d\langle \theta \rangle}{dz} = i\mathcal{E}_x(z)\langle \theta \rangle, \quad (43)$$

and the following coupled equations for $\langle x^2 \rangle$, $\langle \rho \rangle$, and $\langle \sigma \rangle$:

$$\frac{d\langle x^2 \rangle}{dz} = 2\Delta \operatorname{Re}(\langle \sigma \rangle), \quad (44)$$

$$\frac{d\langle \rho \rangle}{dz} = -2i\mathcal{E}_x(z)\langle \rho \rangle + i\mathcal{E}_x(z), \quad (45)$$

$$\frac{d\langle \sigma \rangle}{dz} = 4\Delta\langle \rho \rangle - i\mathcal{E}_x(z)\langle \sigma \rangle. \quad (46)$$

Equation (43) can be readily integrated, yielding the following evolution equation for the beam center of mass:

$$\langle x(z) \rangle = \langle x(0) \rangle + 2 \operatorname{Im}\{q_0\Omega^*(z)\}, \quad (47)$$

where we have set

$$\Omega(z) \equiv \int_0^z d\xi \Delta \exp[-i\phi(\xi)], \quad (48)$$

$$\phi(z) \equiv \int_0^z d\xi \mathcal{E}_x(\xi), \quad (49)$$

$$q_0 \equiv \sum_n c_n^*(0)c_{n+1}(0). \quad (50)$$

Similarly, integration of Eqs. (45) and (46) yields

$$\langle \rho(z) \rangle = \exp[-2i\phi(z)] \left\{ \langle \rho(0) \rangle + \frac{1}{2} \exp[2i\phi(z)] - \frac{1}{2} \right\}, \quad (51)$$

$$\langle \sigma(z) \rangle = \exp[-i\phi(z)] \left\{ \langle \sigma(0) \rangle + 4\Omega(z) \left[\langle \rho(0) \rangle - \frac{1}{2} \right] + 2\Omega^*(z) \right\}. \quad (52)$$

Taking into account that $\Delta \exp[-i\phi(z)] = d\Omega/dz$ and that $2 \operatorname{Re}\{\int_0^z d\xi \Omega^*(\xi)(d\Omega/d\xi)\} = |\Omega(z)|^2$, substitution of Eq. (52) into Eq. (44) yields

$$\langle x^2(z) \rangle = \langle x^2(0) \rangle + 2|\Omega(z)|^2 + 2 \operatorname{Re}\{q_1\Omega(z) - q_2\Omega^2(z)\}, \quad (53)$$

where we have set

$$q_1 \equiv i \sum_n (2n-1)c_n^*(0)c_{n-1}(0), \quad (54)$$

$$q_2 \equiv \sum_n c_n^*(0)c_{n-2}(0). \quad (55)$$

The beam size w_x is then given by

$$w_x(z) = \sqrt{\langle x^2(z) \rangle - \langle x(z) \rangle^2}. \quad (56)$$

For a given field distribution $c_n(0)$ at the input plane, the evolutions of the beam center of mass $\langle x(z) \rangle$ and beam size $w_x(z)$ are thus ruled by Eqs. (47), (53), and (56). Note that beam evolution depends on the input beam parameters q_1 , q_2 , and q_3 —defined by Eqs. (50), (54), and (55)—and by the complex amplitude $\Omega(z)$, defined by Eqs. (48) and (49) and accounting for bending of waveguide axis. Note also that for straight arrays $\Omega(z) = \Delta z$, and one thus retrieves the results of

discrete diffraction derived in Sec. II B, in particular the linear asymptotic increase in w_x with z . The condition for diffraction suppression, i.e., a nonsecular growth of $w_x(z)$ with z , is that $\Omega(z)$ remain a limited function of z as z increases. This condition is always satisfied for a constant value of \mathcal{E}_x , which corresponds to circularly curved waveguides and to the onset of the optical analog of Bloch oscillations [9]. Similarly, for periodic axis bending with spatial period Λ , $\mathcal{E}_x(z)$ is a periodic function of z , and the condition of boundedness of $\Omega(z)$ is given by

$$\int_0^\Lambda d\xi \exp[-i\phi(\xi)] = 0, \quad (57)$$

which is precisely the condition of “dynamic localization” previously investigated in Refs. [12,13].

B. Two-dimensional array

For two-dimensional waveguide array model (38), the moment equations turn out to decouple into two set of equations, similar to Eqs. (42)–(46), separately acting onto the x and y directions. The evolution equations for the beam center of mass $\langle x \rangle, \langle y \rangle$ are then given by

$$\langle x(z) \rangle = \langle x(0) \rangle + 2 \operatorname{Im}\{q_{0x}\Omega_x^*(z)\}, \quad (58)$$

$$\langle y(z) \rangle = \langle y(0) \rangle + 2 \operatorname{Im}\{q_{0y}\Omega_y^*(z)\}, \quad (59)$$

where we have set

$$\Omega_{x,y}(z) = \int_0^z d\xi \Delta_{x,y} \exp[-i\phi_{x,y}(\xi)], \quad (60)$$

$$\phi_{x,y}(z) = \int_0^z d\xi \mathcal{E}_{x,y}(\xi), \quad (61)$$

and

$$q_{0x} = \sum_{n,m} c_{n,m}^*(0)c_{n+1,m}(0), \quad (62)$$

$$q_{0y} = \sum_{n,m} c_{n,m}^*(0)c_{n,m+1}(0). \quad (63)$$

Similarly, the beam sizes w_x and w_y , defined as

$$w_x(z) = \sqrt{\langle x^2(z) \rangle - \langle x(z) \rangle^2}, \quad (64)$$

$$w_y(z) = \sqrt{\langle y^2(z) \rangle - \langle y(z) \rangle^2}, \quad (65)$$

are calculated using Eqs. (58) and (59) and the following evolution equations for $\langle x^2(z) \rangle$ and $\langle y^2(z) \rangle$:

$$\langle x^2(z) \rangle = \langle x^2(0) \rangle + 2|\Omega_x|^2 + 2 \operatorname{Re}\{q_{1x}\Omega_x - q_{2x}\Omega_x^2\}, \quad (66)$$

$$\langle y^2(z) \rangle = \langle y^2(0) \rangle + 2|\Omega_y|^2 + 2 \operatorname{Re}\{q_{1y}\Omega_y - q_{2y}\Omega_y^2\}, \quad (67)$$

where we have set

$$q_{1x} = i \sum_{n,m} (2n-1)c_{n,m}^*(0)c_{n-1,m}(0), \quad (68)$$

$$q_{2x} = \sum_{n,m} c_{n,m}^*(0)c_{n-2,m}(0), \quad (69)$$

$$q_{1y} = i \sum_{n,m} (2m-1)c_{n,m}^*(0)c_{n,m-1}(0), \quad (70)$$

$$q_{2y} = \sum_{n,m} c_{n,m}^*(0)c_{n,m-2}(0). \quad (71)$$

IV. SHAPE-INVARIANT DISCRETE BEAMS

The existence of shape-invariant beams, i.e., families of field distributions that propagate without changing their functional shape, is well known for paraxial propagation in Gaussian optics or in continuous lensguide media (see, for instance, [27]). Here we address the related problem of investigating the existence of shape-invariant discrete beams, i.e., field distributions that do not change their functional shape when propagating along waveguide arrays with arbitrarily curved optical axis. This is a rather challenging problem because no general method capable of constructing shape-invariant beams seems to be available. However, for the simple waveguide array models considered in Sec. III, a family of shape-invariant discrete beams can be introduced in a simple manner. Owing to their functional form, such beams are referred to as discrete Bessel beams.

A. Discrete Bessel beams in one-dimensional arrays

Let us consider a one-dimensional waveguide array with an arbitrarily curved optical axis. In the tight-binding and nearest-neighbor coupling approximations, light propagation is described by the following set of coupled-mode equations:

$$i\dot{c}_n = -\Delta(c_{n+1} + c_{n-1}) - nf(z)c_n, \quad (72)$$

where $f(z)$ describes the rate of transverse index gradient induced by waveguide bending [13], lumped waveguide tilting [3], or locally imposed phase changes among adjacent waveguides [26] as discussed previously. Let us first observe that if $c_n(z)$ is a solution to Eq. (72) corresponding to a given initial field distribution $c_n(0)$, then for an arbitrary integer n_0

$$g_n(z) = c_{n-n_0}(z) \exp\left\{in_0 \int_0^z d\xi f(\xi)\right\} \quad (73)$$

is the solution to Eq. (72) corresponding to the translated initial field distribution $g_n(0) = c_{n-n_0}(0)$. Therefore, apart from an unimportant phase change, shape-invariant beams remain invariant for an arbitrary transverse translation on the lattice.

Let us tentatively search for a solution to Eq. (72) of the form

$$c_n(z) = J_n(\alpha) \exp(-i\sigma n), \quad (74)$$

where J_n is the Bessel function of first kind of order n , and $\alpha = \alpha(z)$ and $\sigma = \sigma(z)$ are unknown functions which depend on propagation distance z , but not on lattice site n . Note that, as $\sum_n n |J_n(\alpha)|^2 = 0$ and $[\sum_n |J_n(\alpha)|^2 n^2] = \alpha^2/2$, the parameter α is related to the beam size w_x [Eq. (6)] by the simple relation

$w_x = \alpha/\sqrt{2}$, whereas σ defines a transverse tilt of the beam “phase front.” Substitution of Eq. (74) into Eq. (72) and taking into account the identities of Bessel functions $J_{n+1}(\alpha) + J_{n-1}(\alpha) = (2n/\alpha)J_n(\alpha)$ and $J_{n-1}(\alpha) - J_{n+1}(\alpha) = 2J'_n(\alpha)$, one obtains that Eq. (74) is indeed a solution to Eq. (72) provided that α and σ satisfy the coupled equations

$$\dot{\alpha} = -2\Delta \sin \sigma, \quad (75)$$

$$\dot{\sigma} = -\frac{2\Delta}{\alpha} \cos \sigma - f. \quad (76)$$

Owing to the functional form of c_n , we will refer such shape-invariant beams to as discrete Bessel beams. Let us define a complex- q parameter for discrete Bessel beam (74) according to

$$q(z) = \alpha(z) \exp[i\sigma(z)], \quad (77)$$

so that the modulus of the complex- q parameter gives the beam spot size at propagation distance z , whereas its phase corresponds to the phase front gradient. From Eqs. (75) and (76) one readily obtains for the complex- q parameter the following simple evolution equation:

$$\frac{dq}{dz} = -2i\Delta - if(z)q. \quad (78)$$

The general solution to Eq. (78), for a given initial value $q(0)$ at the $z=0$ input plane, is given by

$$q(z) = \exp[-i\phi(z)] \left\{ q(0) - 2i \int_0^z d\xi \Delta \exp[i\phi(\xi)] \right\}, \quad (79)$$

where

$$\phi(z) = \int_0^z d\xi f(\xi). \quad (80)$$

The propagation of a discrete Bessel beam along a curved waveguide array is thus reduced to the propagation of its complex- q parameter, which plays an analogous role of the complex- q parameter for Gaussian beams in lensguide media. The propagation law of the q parameter admits a simple geometrical interpretation in the complex- q plane. According to Eq. (78), for an infinitesimal propagation distance δz the change in $q(z)$ is given by the superposition of the two paths AB and BC shown in Fig. 2(a). Path AB, of length $2\delta z\Delta$, accounts for discrete diffraction and corresponds to a change in $q(z)$ along the imaginary q axis. Path BC is due to the transverse index gradient which produces a clockwise rotation by the angle $\delta\gamma = f(z)\delta z$ around origin O of the complex plane. It is interesting to note that, since $J_n(0) = \delta_{n,0}$, for $q(0) = 0$ the discrete Bessel beam [Eq. (74)] reduces to the well-known impulse response of a tight-binding array with nearest-neighbor couplings (see, for instance, [33]).

To appreciate the usefulness of the q -parameter description and some properties of discrete Bessel beams, let us now discuss a few examples and applications.

Propagation of discrete Bessel beams in homogeneous ar-

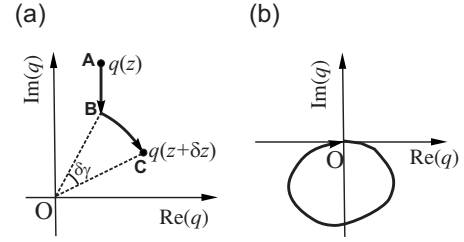


FIG. 2. (a) Geometric construction of the evolution of the complex- q parameter for an infinitesimal propagation distance δz . The length of segment AB is $2\Delta\delta z$, whereas the rotation angle is $\delta\gamma = f(z)\delta z$. Points A and C correspond to $q(z)$ and $q(z + \delta z)$, respectively. (b) Geometric representation of a self-imaging array: the path followed by the complex parameter $q(z)$, starting from origin O, is closed.

rays. For a homogeneous array ($f=0$), the propagation law of the complex- q parameter is simply given by

$$q(z) = q(0) - 2i\Delta z. \quad (81)$$

If we assume, for the sake of definiteness, that at the input plane $z=0$ the phase front of the beam is flat, i.e., $q(0) = \alpha(0) = \alpha_0$ is real valued, the following propagation laws for beam size α and beam phase tilt σ are derived:

$$\alpha(z) = \alpha_0 \sqrt{1 + \left(\frac{2\Delta z}{\alpha_0}\right)^2}, \quad (82)$$

$$\sigma(z) = -\arctan\left(\frac{2\Delta z}{\alpha_0}\right). \quad (83)$$

From Eq. (82) we may introduce, as for Gaussian beams propagating in free space [27], the Rayleigh range z_R and divergence angle θ_d such that $\alpha(z_R) = \sqrt{2}\alpha_0$ and $\theta_d = \lim_{z \rightarrow \infty} \alpha(z)/z$, i.e.,

$$z_R = \frac{\alpha_0}{2\Delta}, \quad (84)$$

$$\theta_d = 2\Delta. \quad (85)$$

It should be noted that, as opposed to the case of Gaussian beams in free space—for which the Rayleigh range z_R is proportional to the *square* of the spot size α_0 at the beam waist and the diffraction angle θ_d is inversely proportional to α_0 —for discrete Bessel beams the Rayleigh range z_R is proportional to the spot size α_0 at the beam waist, whereas the divergence angle is *independent* of the beam spot size and always equal to the diffraction cone angle introduced in Sec. II D. This peculiar property is closely related to the very general result, proven in Sec. II D, that the far field of discrete diffraction in a homogenous waveguide array is peaked at the observation angles corresponding to the flattest points (self-collimation points) of the band dispersion curve.

Transformation of a discrete Bessel beam through a waveguide axis tilt. A tilt of the waveguide axis at $z=z_0$ by a (small) angle θ corresponds to impressing a phase shift

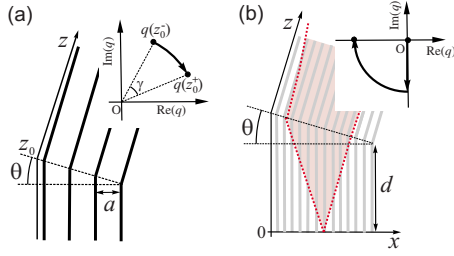


FIG. 3. (Color online) (a) Schematic of a one-dimensional waveguide array with a tilt of waveguide axis at $z=z_0$, and the transformation induced on the complex- q parameter by the tilt (inset). (b) Principle of beam collimation via waveguide axis tilt [tilt angle $\theta=\lambda/(4an_s)$], and path followed by the complex- q parameter for single waveguide input excitation from $z=0$ to $z=d^*$ (inset).

$$\gamma = \frac{2\pi}{\lambda} a \theta n_s \quad (86)$$

between adjacent waveguides, where a is the waveguide spacing and n_s is the effective index of propagating modes [see Fig. 3(a)]. Light propagation across the tilt can be thus modeled by assuming $f(z)=\gamma\delta(z-z_0)$ in Eq. (72), and its effect on the complex- q parameter is to produce a rotation around the origin of the complex plane by an angle γ [see the inset of Fig. 3(a)].

A tilt of the waveguide axis may be used to “collimate” a discrete beam, as schematically shown in Fig. 3(b). Here a single waveguide is initially excited at the input plane, and after a propagation distance d the axis of the array is tilted by an angle $\theta=\lambda/(4an_s)$ such that $\gamma=\pi/2$. The 90° rotation of the q parameter in the complex plane due to axis bending [see the inset of Fig. 3(b)] brings the q parameter on the real axis, with a zero phase gradient $\sigma=0$ and an enlarged beam size $\alpha=2\Delta d$. The axis tilt thus plays a similar role of a collimating lens for a diverging Gaussian beam. Note however that, contrary to a conventional lens, the tilting angle θ for achieving beam collimation is independent of the distance d between source point (at $z=0$) and the lens plane ($z=d$). Figure 4 shows an example of beam collimation in a 6-cm-long one-dimensional array as obtained by numerical analysis of the scalar wave equation for the electric field envelope $E(x,z)$ propagating in the structure based on a standard beam propagation method. Figure 4(a) shows a pseudocolor map of the intensity beam evolution $|E(x,z)|^2$ along the structure when a single waveguide is excited in its fundamental mode at the input plane $z=0$ and the waveguide axis is tilted at a distance $d=2$ cm from the input plane [horizontal dotted curve in Fig. 4(a)]. The refractive index profile $n(x)$ used in the simulations is depicted in Fig. 4(b), and the values of other parameters are $\lambda=1.55 \mu\text{m}$, $n_s=1.52$, and $a=11 \mu\text{m}$, corresponding to a tilting angle $\theta=\lambda/(4an_s)\approx 23.2$ mrad. For the sake of readability, the intensity distribution is plotted with the waveguide axis z unfolded along a straight line. Note that the numerical results provide a realistic behavior of beam propagation beyond the coupled-mode equation approximation, accounting for radiation losses and coupling to higher-order bands due to axis bending. These latter effects, however, are very small for the parameter values adopted in

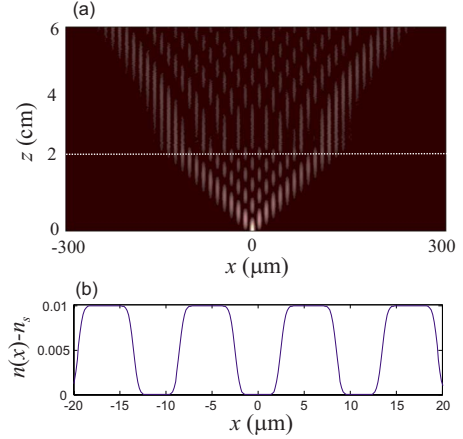


FIG. 4. (Color online) (a) Pseudocolor map of beam intensity propagation in a waveguide array with one axis tilting as obtained by numerical simulations, showing beam collimation. (b) Refractive index profile of the waveguide array used in the numerical simulations. The values of other parameters are given in the text.

the simulations, and the coupled-mode equation model works fine.

Geometric interpretation of the self-imaging condition and polygonal Bloch oscillations. An array of length d shows a self-imaging property (also referred to as diffraction cancellation or dynamic localization) whenever $|c_n(d)|^2 = |c_n(0)|^2$ for any initial field distribution. The dynamic localization condition has a rather simple geometric interpretation in the complex- q plane. In fact, if the array is excited in waveguide $n=0$, $q(0)=0$ and to achieve self-imaging after a propagation distance d one necessarily has to have $q(d)=q(0)=0$, i.e., the path described by the complex- q parameter, starting from origin O of the complex plane, should be closed [see Fig. 2(b)]. Owing to the translational invariance of discrete Bessel beams [Eq. (73)], this condition is also sufficient. From Eq. (79), the closed-path condition $q(d)=q(0)=0$ yields

$$\int_0^d dz \exp[i\phi(z)] = 0, \quad (87)$$

which is precisely the condition for dynamic localization derived originally by Dunlap and Kenkre in Ref. [33].

An application of the geometric condition of dynamic localization is that of polygonal Bloch oscillations. Let us consider a waveguide array whose axis forms an (open) polygonal curve of large (mean) radius R made of a sequence of straight segments of same length b and with tilt angle θ , as shown in Fig. 5(a). The function $\phi(z)$, defined by Eq. (80), is thus a staircase function, which increases in steps of $\gamma=(2\pi/\lambda)a\theta n_s$ [see Eq. (86)] at $z=b, 2b, 3b, \dots$ (the coordinate z is measured along the polygonal curve). After a propagation $d=(N+1)b$ from the input $z=0$ plane, where N is an integer number, it then follows that

$$\int_0^d dz \exp[i\phi(z)] = b \sum_{n=0}^N \exp(i\gamma n). \quad (88)$$

The sum of complex numbers (phasors) on the right-hand side of Eq. (88) can be obtained analytically and has a well-

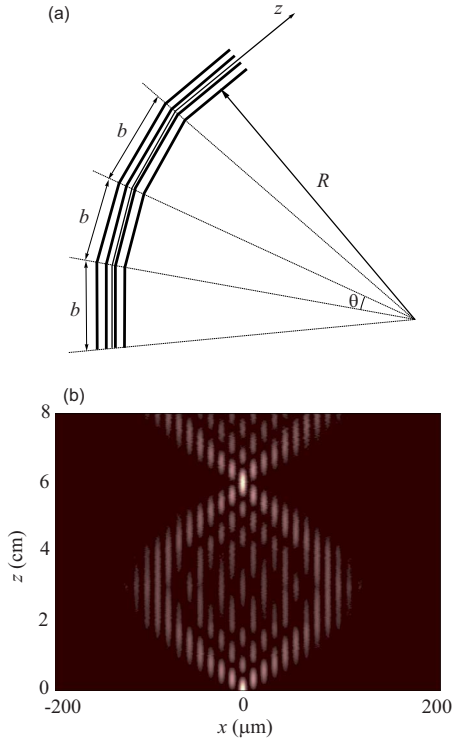


FIG. 5. (Color online) (a) Schematic of a polygonal waveguide array for the observation of Bloch oscillations. (b) Pseudocolor image of beam intensity propagation in a 8-cm-long polygonal array showing a Bloch oscillation breathing mode. The refractive index profile of the waveguide array used in the numerical simulations is the same as in Fig. 4(b). The values of other parameters are given in the text.

known geometric interpretation. In particular, if γ satisfies the condition $\gamma = 2\pi/(N+1)$, i.e., if the tilt angle θ is given by

$$\theta = \frac{\lambda}{an_s(N+1)}, \quad (89)$$

the sum on the right-hand side of Eq. (88) vanishes, and the condition for self-imaging is attained. An example of the self-imaging property of a polygonal waveguide array is shown in Fig. 5(b) for the case $N=5$. The figure depicts a characteristic breathing mode corresponding to a single waveguide excitation at the input plane. The waveguide array parameters are the same as in Fig. 4, and a sequence of axis tilts are placed at distances $b=1$ cm one to the next. The tilt angle θ , chosen according to Eq. (89), is $\theta \approx 15.5$ mrad, yielding a self-imaging plane at $d=(N+1)b=6$ cm, as clearly shown in Fig. 5(b). Note that in the limit $b \rightarrow 0$, $N \rightarrow \infty$, and $b/\theta \rightarrow R$ finite, the polygonal of Fig. 5(a) approximates an arc of a circumference of radius R , and condition (89) for self-imaging is satisfied for a propagation distance

$$d = (N+1)b \rightarrow \frac{\lambda R}{n_s a}, \quad (90)$$

which is the spatial period of Bloch oscillations on a curved waveguide array (radius of curvature R) previously consid-

ered in Refs. [9,10]. The usual Bloch oscillations on a curved waveguide array may be therefore viewed as a limiting case of Bloch oscillations on a polygonal array.

B. Discrete Bessel beams in two-dimensional arrays

A simple extension of the analysis of Sec. IV A can be done for a two-dimensional rectangular-lattice waveguide array with nearest-neighbor coupling when the diagonal coupling is neglected. This model is described by the coupled-mode equation

$$i\dot{c}_{n,m} = -\Delta_x(c_{n+1,m} + c_{n-1,m}) - \Delta_y(c_{n,m+1} + c_{n,m-1}) - f_x(z)nc_{n,m} - f_y(z)mc_{n,m}, \quad (91)$$

where $f_{x,y}(z)$ describe the rates of transverse index gradients induced by waveguide bending or lumped waveguide axis tilting along the x and y directions. Since Eq. (91) admits separable solutions $c_{n,m}(z) = c_n(z)c_m(z)$, with $c_n(z)$ and $c_m(z)$ as solutions to one-dimensional problem (72) with $\Delta = \Delta_{x,y}$ and $f(z) = f_{x,y}(z)$, a two-dimensional discrete Bessel beam has the form

$$c_{n,m}(z) = J_n(\alpha_x)J_m(\alpha_y)\exp(-i\sigma_x n - \sigma_y m). \quad (92)$$

The complex- q parameters of the beam along the x and y directions are defined by

$$q_x(z) = \alpha_x(z)\exp[i\sigma_x(z)], \quad q_y(z) = \alpha_y(z)\exp[i\sigma_y(z)], \quad (93)$$

and their evolution is ruled out by the equation

$$\dot{q}_{x,y} = -2i\Delta_{x,y} - if_{x,y}(z), \quad (94)$$

which has a similar geometric interpretation as that discussed in Sec. IV A. The propagation properties of two-dimensional discrete Bessel beams in homogeneous arrays, across tilted axis regions or polygonal curves, are the same as those investigated for one-dimensional beams, and are therefore not further discussed here.

V. CONCLUSIONS

In this paper, a comprehensive study of discrete diffraction and linear propagation of light in homogeneous and curved waveguide arrays has been presented. In particular, general laws describing beam spreading, beam decay, and discrete far-field patterns in homogeneous arrays have been derived using the method of moments and the steepest-descent method, and some remarks on the well-known self-collimation regime have been pointed out. In curved arrays and within the nearest-neighbor coupling approximation, the method of moments has been extended to describe the evolution of global beam parameters. This method provides an alternative means to algebraic operator techniques recently proposed in other physical contexts to study general properties of Bloch oscillations [28–30]. Finally, a family of shape-invariant discrete beams—referred to as discrete Bessel beams owing to their functional form—has been introduced. It has been shown that propagation of such beams in curved

waveguide arrays is simply described by the evolution of a complex- q parameter, which plays a similar role to the complex- q parameter used for Gaussian beams in continuous lensguide media. A few applications of the q parameter formalism are discussed, including beam collimation via waveguide axis tilting, a geometric interpretation of the self-imaging effect in waveguide arrays, and optical Bloch oscillations on a polygonal array.

malism are discussed, including beam collimation via waveguide axis tilting, a geometric interpretation of the self-imaging effect in waveguide arrays, and optical Bloch oscillations on a polygonal array.

-
- [1] D. N. Christodoulides, F. Lederer, and Y. Silberberg, *Nature (London)* **424**, 817 (2003).
- [2] F. Lederer, G. I. Stegeman, D. N. Christodoulides, G. Assanto, M. Segev, and Y. Silberberg, *Phys. Rep.* **463**, 1 (2008).
- [3] H. S. Eisenberg, Y. Silberberg, R. Morandotti, and J. S. Aitchison, *Phys. Rev. Lett.* **85**, 1863 (2000).
- [4] T. Pertsch, T. Zentgraf, U. Peschel, A. Bräuer, and F. Lederer, *Phys. Rev. Lett.* **88**, 093901 (2002).
- [5] R. Iwanow, D. A. May-Arrijo, D. N. Christodoulides, G. I. Stegeman, Y. Min, and W. Sohler, *Phys. Rev. Lett.* **95**, 053902 (2005).
- [6] A. Szameit, F. Dreisow, H. Hartung, S. Nolte, A. Tünnermann, and F. Lederer, *Appl. Phys. Lett.* **90**, 241113 (2007).
- [7] U. Peschel, T. Pertsch, and F. Lederer, *Opt. Lett.* **23**, 1701 (1998).
- [8] R. Morandotti, U. Peschel, J. S. Aitchison, H. S. Eisenberg, and Y. Silberberg, *Phys. Rev. Lett.* **83**, 4756 (1999); T. Pertsch, P. Dannberg, W. Elflein, A. Bräuer, and F. Lederer, *ibid.* **83**, 4752 (1999).
- [9] G. Lenz, I. Talanina, and C. M. de Sterke, *Phys. Rev. Lett.* **83**, 963 (1999).
- [10] B. A. Usievich, V. A. Sychugov, J. Kh. Nirligareev, and K. M. Golant, *Opt. Spectrosc.* **97**, 790 (2004); N. Chiodo, G. Della Valle, R. Osellame, S. Longhi, G. Cerullo, R. Ramponi, P. Laporta, and U. Morgner, *Opt. Lett.* **31**, 1651 (2006); H. Trompeter, T. Pertsch, F. Lederer, D. Michaelis, U. Streppe, A. Bräuer, and U. Peschel, *Phys. Rev. Lett.* **96**, 023901 (2006); H. Trompeter, W. Krolikowski, D. N. Neshev, A. S. Desyatnikov, A. A. Sukhorukov, Yu. S. Kivshar, T. Pertsch, U. Peschel, and F. Lederer, *ibid.* **96**, 053903 (2006).
- [11] A. Szameit, T. Pertsch, S. Nolte, A. Tünnermann, U. Peschel, and F. Lederer, *J. Opt. Soc. Am. B* **24**, 2632 (2007).
- [12] G. Lenz, R. Parker, M. C. Wanke, and C. M. de Sterke, *Opt. Commun.* **218**, 87 (2003); J. Wan, M. Laforest, C. M. de Sterke, and M. M. Dignam, *ibid.* **247**, 353 (2005).
- [13] S. Longhi, *Opt. Lett.* **30**, 2137 (2005); S. Longhi, M. Marangoni, M. Lobino, R. Ramponi, P. Laporta, E. Cianci, and V. Foglietti, *Phys. Rev. Lett.* **96**, 243901 (2006); S. Longhi, M. Lobino, M. Marangoni, R. Ramponi, P. Laporta, E. Cianci, and V. Foglietti, *Phys. Rev. B* **74**, 155116 (2006); R. Iyer, J. S. Aitchison, J. Wan, M. M. Dignam, and C. M. de Sterke, *Opt. Express* **15**, 3212 (2007); F. Dreisow, M. Heinrich, A. Szameit, S. Döring, S. Nolte, A. Tünnermann, S. Fahr, and F. Lederer, *ibid.* **16**, 3474 (2008).
- [14] I. L. Garanovich, A. A. Sukhorukov, and Y. S. Kivshar, *Phys. Rev. E* **74**, 066609 (2006); I. L. Garanovich, A. A. Sukhorukov, and Y. S. Kivshar, *Opt. Express* **15**, 9547 (2007); I. L. Garanovich, *Phys. Lett. A* **372**, 3922 (2008).
- [15] I. L. Garanovich, A. Szameit, A. A. Sukhorukov, T. Pertsch, W. Krolikowski, S. Nolte, D. Neshev, A. Tünnermann, and Y. S. Kivshar, *Opt. Express* **15**, 9737 (2007).
- [16] M. J. Ablowitz and Z. H. Musslimani, *Phys. Rev. Lett.* **87**, 254102 (2001); A. Szameit, I. L. Garanovich, M. Heinrich, A. Minovich, F. Dreisow, A. A. Sukhorukov, T. Pertsch, D. N. Neshev, S. Nolte, W. Krolikowski, A. Tünnermann, A. Mitchell, and Y. S. Kivshar, *Phys. Rev. A* **78**, 031801(R) (2008).
- [17] K. G. Makris and D. N. Christodoulides, *Phys. Rev. E* **73**, 036616 (2006); S. Longhi, *ibid.* **74**, 026602 (2006); A. Szameit, T. Pertsch, F. Dreisow, S. Nolte, A. Tünnermann, U. Peschel, and F. Lederer, *Phys. Rev. A* **75**, 053814 (2007).
- [18] R. Iwanow, R. Schiek, G. I. Stegeman, T. Pertsch, F. Lederer, Y. Min, and W. Sohler, *Phys. Rev. Lett.* **93**, 113902 (2004); S. Suntsov, K. G. Makris, D. N. Christodoulides, G. I. Stegeman, A. Hache, R. Morandotti, H. Yang, G. Salamo, and M. Sorel, *ibid.* **96**, 063901 (2006); Y. V. Kartashov, V. A. Vysloukh and L. Torner, *ibid.* **96**, 073901 (2006); M. Molina, Y. Kartashov, L. Torner, and Y. Kivshar, *Opt. Lett.* **32**, 2668 (2007); A. Szameit, Y. V. Kartashov, F. Dreisow, T. Pertsch, S. Nolte, A. Tünnermann, and L. Torner, *Phys. Rev. Lett.* **98**, 173903 (2007); X. Wang, A. Bezryadina, Z. Chen, K. G. Makris, D. N. Christodoulides, and G. I. Stegeman, *ibid.* **98**, 123903 (2007).
- [19] I. L. Garanovich, A. A. Sukhorukov, and Y. S. Kivshar, *Phys. Rev. Lett.* **100**, 203904 (2008); A. Szameit, I. L. Garanovich, M. Heinrich, A. A. Sukhorukov, F. Dreisow, T. Pertsch, S. Nolte, A. Tünnermann, and Yu. S. Kivshar, *ibid.* **101**, 203902 (2008).
- [20] H. Kosaka, T. Kawashima, A. Tomita, M. Notomi, T. Tammura, T. Sato, and S. Kawakami, *Appl. Phys. Lett.* **74**, 1212 (1999); J. Witzens, M. Loncar, and A. Scherer, *IEEE J. Sel. Top. Quantum Electron.* **8**, 1246 (2002); Z. Lu, S. Shi, J. A. Murakowski, G. J. Schneider, C. A. Schuetz, and D. W. Prather, *Phys. Rev. Lett.* **96**, 173902 (2006); P. T. Rakich, M. S. Dahlem, S. Tandon, M. Ibanescu, M. Soljacic, G. S. Petrich, J. D. Joannopoulos, L. A. Kolodziejski, and E. P. Ippen, *Nature Mater.* **5**, 93 (2006).
- [21] See, for instance, J. M. Ziman, *Principles of the Theory of Solids*, 2nd ed. (Cambridge University Press, Cambridge, 1979).
- [22] S. G. Krivoshlykov, *Quantum-Theoretical Formalism for Inhomogeneous Graded-Index Waveguides* (Akademie-Verlag, Berlin, 1994).
- [23] J. R. Klein, *Am. J. Phys.* **48**, 1035 (1980); D. F. Styer, *ibid.* **58**, 742 (1990); P. A. Bélanger, *Opt. Lett.* **16**, 196 (1991); V. M. Pérez-García, P. Torres, J. J. García-Ripoll, and H. Michinel, *J. Opt. B: Quantum Semiclassical Opt.* **2**, 353 (2000); S. Longhi, G. Della Valle, and D. Janner, *Phys. Rev. E* **69**, 056608 (2004); A. K. Potemkin and E. A. Khazanov, *Quantum Electron.* **35**, 1042 (2005).
- [24] F. W. J. Olver, *Asymptotics and Special Functions* (Academic, New York, 1974).
- [25] It should be noted that for special initial field distributions with low decaying tails, yet carrying a finite power, the spectrum

- $F(k)$ may diverge, and the decay law may be slower than $\sim 1/\sqrt{z}$ [see K. Unnikrishnan, *Am. J. Phys.* **65**, 526 (1997); F. Lillo and R. N. Mantegna, *Phys. Rev. Lett.* **84**, 1061 (2000)]. This curious circumstance happens, for instance, for beams with power-law decay tails. However, for such special beams the moment $\langle x^2 \rangle$ is unbounded. In this paper we will limit ourselves to consider beams with a bounded variance, for which the corresponding spectrum $F(k)$ is not singular.
- [26] A. Szameit, F. Dreisow, M. Heinrich, T. Pertsch, S. Nolte, A. Tünnermann, E. Suran, F. Louradour, A. Barthélémy, and S. Longhi, *Appl. Phys. Lett.* **93**, 181109 (2008).
- [27] A. E. Siegman, *Lasers* (University Science, Mill Valley, CA, 1986).
- [28] H. L. Haroutyunyan and G. Nienhuis, *Phys. Rev. A* **64**, 033424 (2001).
- [29] H. J. Korsch and S. Mossmann, *Phys. Lett. A* **317**, 54 (2003).
- [30] S. Mossmann, A. Schulze, D. Witthaut, and H. J. Korsch, *J. Phys. A* **38**, 3381 (2005).
- [31] T. Pertsch, U. Peschel, F. Lederer, J. Burghoff, M. Will, S. Nolte, and A. Tünnermann, *Opt. Lett.* **29**, 468 (2004).
- [32] Analytical results can be also provided for a more general two-dimensional lattice model, in which nearest diagonal coupling terms are accounted for in Hamiltonian (38) (see Ref. [30]). However, the resulting equations are very cumbersome, and this case will not be considered here.
- [33] D. H. Dunlap and V. M. Kenkre, *Phys. Rev. B* **34**, 3625 (1986).